Full Length Article

Development of a cooperative system for wire and arc additive manufacturing and machining

Hideaki Nagamatsu[a,*], Hiroyuki Sasahara[a,*], Yuusuke Mitsutake[b], Takeshi Hamamoto[b]

[a] Department of Mechanical Systems Engineering, Tokyo University of Agriculture and Technology, 2-24-16 Naka-cho, Koganei City, Tokyo, 184-8588, Japan
[b] MUTOH INDUSTRIES LTD., 3-1-3 Ikejiri, Setagaya-ku, Tokyo, 154-8560, Japan

ARTICLE INFO

ABSTRACT

Wire and arc additive manufacturing (WAAM), which is an additive manufacturing (AM) process that uses metal materials, has a higher fabricated volume per unit time but a lower fabricated shape accuracy compared with other methods. With this process, the surface roughness of fabricated objects is several hundred micrometers or more, and a finishing process is necessary. However, the fabricated objects after finishing can have uncut areas or can be overcut during the finishing process owing to the large difference between the target and actual fabricated shapes. Therefore, the objective of this study is to develop a cooperative system for WAAM and machining that includes a process that measures the shape of the fabricated object. First, the three-dimensional (3-D) shape of the fabricated object was measured by structure from motion (SfM) and compared with the 3-D computer-aided design (CAD) data. Second, the original design was modified, and the amount of material removed during finish cutting was optimized with the developed software. Finally, the fabricated hollow object was finished by milling to obtain a uniform wall thickness without any defects. A 3-D fabricated object was measured by SfM, and it was observed that the measurement accuracy was sufficiently high for the requirements of the system. In addition, a fabricated hollow quadrangular pyramid with a closed shape was machined with a computer numerical control (CNC) machine tool with the modification of the work origin. As a result, the amount of material removed during finish cutting was optimized, and the inclined wall thickness was uniform compared with that without modification. In addition, a hollow turbine blade with a freeform shape was successfully finished without any defects.

1. Introduction

Wire and arc additive manufacturing (WAAM) is classified as directed energy deposition (DED) and uses wire as a material and an arc discharge as an energy source [1]. Compared with powder and laser-based additive manufacturing (AM) process, WAAM has a few advantages. First, WAAM systems are considerably more inexpensive and can be configured more simply. Second, the WAAM process can handle various metallic materials with metal inert gas (MIG)/metal active gas (MAG) welding technology [2–5]. Third, the energy efficiency of wire and arc-based DED ranges from 75% to 90% depending on the metal and shielding gas, and it is higher than that of powder and laser-based DED, which is 30%–50% [6–8].

In the WAAM process, the fabricated volume per unit length is relatively large owing to the accumulation of the welding bead by MIG/MAG welding. There is a step between each layer, and the surface roughness of a fabricated object is several hundred micrometers or

more. To produce machine parts with a higher precision, it is necessary to develop a system that combines cutting and automation to finish machining from fabrication. There are two possible processes for achieving this goal. The first is to use multitasking machining for both fabrication and cutting. The other is to move fabricated objects on a palette to machine tools after fabrication with a special-purpose fabrication machine. Additionally, DED is believed to be installed in more than half of the commercially available metal hybrid computer numerical control (CNC) systems [1]. The fabrication process requires that the fabrication conditions should satisfy the following: there are no welding defects, and the fabricated object includes the target and is machined without overcutting and any remaining uncut regions.

In contrast, there are some issues related to the control of the fabricated shape in the WAAM process. A near-net-shape structure cannot be fabricated by only controlling the welding torch at an equal speed along thin horizontal cross sections from three-dimensional (3-D) computer-aided design (CAD) data divided into contour lines. For high-

---

quality deposition, it is very important to understand the metallurgical properties and the performance of the construction [9]. Since the phenomena of melting and resolidification occur every layer owing to the high-temperature gradient during the arc discharge, the molten metal pool has a high fluidity on the fabricated object. In a continuous fabrication process that maintains a high build efficiency, the temperature of the fabricated object increases layer by layer, and the solidification rate of the molten metal decreases. In addition, the molten metal on an overhang is influenced by gravity [10]. Consequently, the molten metal solidifies while spilling from the previous layer, and the precision of the shape tends to deteriorate. The influence of the deposition conditions on the shape of the deposited object in the WAAM process has been numerically investigated [11], and the shape of the fabricated object has been geometrically simulated by simplifying the formation of a welding bead [12–14]. These simulations allow the fabricated shape to be observed on a display before fabrication. Therefore, a fabricated object with a simple shape has a sufficiently improved accuracy that includes the target shape. However, there is a limit on the improvement in the simulation accuracy. In particular, for a complicated shape, the difference between the simulated and fabricated shapes is large. Moreover, the thickness of each wall after machining can be uneven owing to thermal deformation. As a result, a process that can guarantee that a target shape is enclosed within a fabricated object, modify the original design, and optimize the amount of material removed during finish cutting is paramount.

To establish an advanced WAAM process, it is important to find a precise measurement method for the WAAM-fabricated shape. This measurement method should satisfy the following conditions: it is desirable to apply a noncontact method because the target object may have an unpredictable shape, and it should be possible to employ one-machine measurement for multitasking machining. In this study, a photogrammetric survey method was carried out for the WAAM process, termed "structure from motion (SfM)." An SfM method can simultaneously estimate the camera pose and scene geometry using a highly redundant bundle adjustment based on matching features in multiple overlapping offset images [15]. Although the basic principles are common to photographic measurements, it is not necessary to calibrate the inside and outside parameters of the camera used, and the 3-D structure can almost be automatically reconstructed. Moreover, SfM only requires a single camera and dedicated software. Thus, the cost is much lower than that of other methods, and it can be employed for one-machine measurement.

In addition to a noncontact measurement method, it is also important to develop a method to modify the work origin. The thicknesses of all of the side walls of a fabricated object can be set to be the same as a target amount by finishing both surfaces of the walls, even if WAAM-fabricated objects do not have a high shape accuracy. However, without a method to modify the work origin properly, machining defects might occur after the finishing process in the following cases.

Case 1: The surfaces of shell structures with thin walls or fabricated objects should be machined close to the target shape.

Case 2: The inner wall of a closed shape cannot be machined because a cutting tool cannot approach an inner wall.

Case 3: Inner walls with complicated shapes cannot be machined. (e.g., valve pipes, turbine blades with twisted shapes, etc.).

For Cases 2 and 3, misalignment of the work origin may cause cutting defects and an uneven wall thickness since the inner walls cannot be machined. One solution is to use a hybrid machine tool that can alternately carry out the cutting and fabricating processes. However, the cost of introducing a hybrid manufacturing machine is high. In particular, the use of a hybrid machine tool is overspecific when manufacturing a hollow shape that does not require a sufficiently high accuracy or low surface roughness compared with that for finishing with the intent of reducing the material consumption or product weight. Hence, a method that modifies the work origin and makes the thickness of each side wall uniform was developed in this study. Furthermore, a WAAM system corresponding to Cases 1–3 was constructed by developing specialized software.

In WAAM that requires a finishing process, the final product shape is classified into the following two patterns.

Case A: The substrate is completely removed after the WAAM process, and only the WAAM-fabricated object becomes the final product after finish machining.

Case B: The existing product on which the WAAM product is fabricated is also handled as a final product.

In the WAAM process, the origin of fabrication is determined with reference to the substrate. Therefore, the product after finishing shifts by the amount of modification from the reference position of the origin of the substrate if the machining origin is modified. In Case A, the substrate is completely removed; thus, the relative position between the substrate and the fabricated object has no influence on the final product shape. In contrast, in Case B, both the fabricated object and existing product have to be cut in a finishing process because the relative position between the existing product and the fabricated object is important. Therefore, it is necessary to prepare an existing product that is larger than the target shape. When the existing product has a complex shape, the work origin should not be modified because it takes long manufacturing time. For these reasons, the proposed WAAM system was developed to be applied to Cases A and B.

The objectives of the present study is to develop a cooperative system for WAAM and machining and to demonstrate that this system can manufacture objects with freeform surfaces. The proposed system comprises mainly four processes: WAAM process, shape measuring and modeling process by SfM for a fabricated object, modification of work origin, and finishing process. The details of each process are provided in section 2.1. First, the fabricated object was measured by SfM, and the relationship between the average accuracy measured by SfM and the number of images for SfM was investigated. Then, the external walls of a fabricated object classified as case 2 were finished using the proposed system. After finishing, the amount of removal cutting and the actual thickness of the inclined walls were measured to verify whether work origin could be modified to ensure that the thickness was constant. Finally, the proposed system was adopted to fabricate and finish a turbine blade with freeform surfaces without any defects.
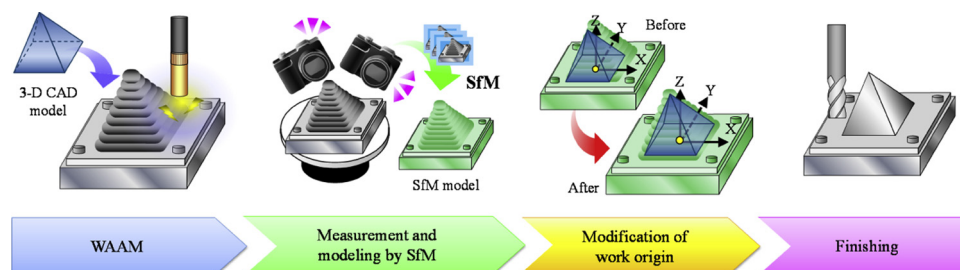

Fig. 1. Cooperative system for WAAM.

2. Experimental methods

2.1. Cooperative system for WAAM and machining

Fig. 1 shows the proposed cooperative system. First, the desired object is fabricated as a near-net shape as much as possible, leaving a small amount of material to be removed during finish cutting. Second, the 3-D shape of the fabricated object is measured by SfM and compared with the 3-D CAD data. Third, the original design is modified, and the amount of material to be removed is optimized for finish cutting. A software for correcting the uniformity of the wall thickness was developed. Finally, the precision machine part can be finished without any defects. WAAM process, SfM process, and the developed software are described in sections 2.2, 2.3, and 2.4, respectively. The proposed system does not include a process to control thermal deformation and the residual stress of fabricated object and substrate material.

In this study, WAAM, SfM, and finishing process were performed using different equipment. To unify a work coordinate, fabricated objects were accumulated on a substrate fixed on a reference blck with thickness of approximately 35 mm, side length of approximately 155 mm, and parallelism and perpendicularity of approximately 1 μm. The corner of this reference block was defined as the work origin in WAAM and SfM process. In the finishing process, the work origin was moved parallelly according to the modified work origin obtained by the developed software.

2.2. WAAM process

2.2.1. WAAM system

Fig. 2 shows the WAAM machine. The WAAM system mainly consists of a CNC machine, control system, deposition system, and cooling unit. It can provide control along three axes (X, Y, and Z) and around a tilt axis (B axis) by the CNC software, Mach2. The strokes along the X, Y, Z, and B axes are 400 mm, 300 mm, 150 mm, and ± 90°, respectively. A welding torch is attached along the Z axis. A substrate or block on which the object is to be accumulated is fixed to the base plate on the table. The deposition system consists of an MIG/MAG heat resource, a wire feeder, a welding torch, and assist gas. The adopted MIG/MAG heat source (DAIHEN Welbee P500 L power supply) can deposit mild steel with preset welding parameters that are automatically adjusted. This heat may decrease the accuracy of the manufactured shape. In particular, it decreases the accuracy of the fabricated shape. To prevent this, a water-cooling tank is incorporated as part of the WAAM machine, and the fabricated object, base block, and B axis are cooled with water. During fabrication, fabricated objects are cooled by manual adjustment of the water level to about 20 mm between the fabrication point and the water surface.

2.2.2. Wire and base materials

In this experiment, mild steel was used as the wire and substrate

Table 1
Fabrication conditions.

Welding machine			P500L
Welding mode			DC low sputtering
Current		A	60
Voltage		V	15
Feed speed		mm/min	100
Wire feed speed		m/min	1.3
Wire material			Equivalent of SS400
Wire diameter		mm	1.2
Substrate	Material		SS400
	Thickness	mm	5, 10
Shielding gas	Ar	%	80
	CO_2	%	20
Shielding gas flow rate		L/min	10
Cooling method			Water cooling

material because of its good weldability and machinability. SE-A50 (φ = 1.20 ± 0.01 mm; Kobe Steel Co., Ltd.) was used as welding wire. The processing conditions are listed in Table 1.

2.3. SfM process

2.3.1. Processing procedure of SfM

SfM is a low-cost and user-friendly photogrammetric technique for the automatic reconstruction of both the 3-D structure of the target shape and the camera poses from multiple images. The major areas of SfM application include photogrammetry for geoscience, the promotion of cultural heritage sites, localization devices for robotic vehicles, and so on [16]. The target objects in these investigations are very large. However, there is not much research on the measurement accuracy of SfM for metal objects that are roughly the size of a cube with a side length of 100 mm. In this study, the objects fabricated with the WAAM process were measured by SfM. Then, the accuracy of the SfM measurements was compared with that measured by a contact-type 3-D measuring machine with a probe.

In this study, a commercial software package (Agisoft Photoscan Professional 1.2.4 (64-bit)) was used as the SfM software. Fig. 3 shows all of the SfM processes in this software package. In the first step, multiple photographs that overlap 60% or more are acquired from different positions using a camera with over 10 million pixels. Feature points are extracted from these photographs by a scale-invariant feature transform (SIFT) or speeded-up robust features (SURF)—the method for image feature generation (Fig. 3(a)). Second, the 3-D coordinates of each feature point and the camera position are estimated by bundle adjustment, factorizing the matrix with the correspondence relationships of the feature points. Third, a "sparse point cloud" is obtained from the 3-D coordinates on the surface of the target object based on them (Fig. 3(b)). Fourth, a "dense point cloud" is generated by calculating the 3-D coordinates of each pixel. Finally, a 3-D shape model with mesh data can be created from the "dense point cloud" (Fig. 3(c)). SfM
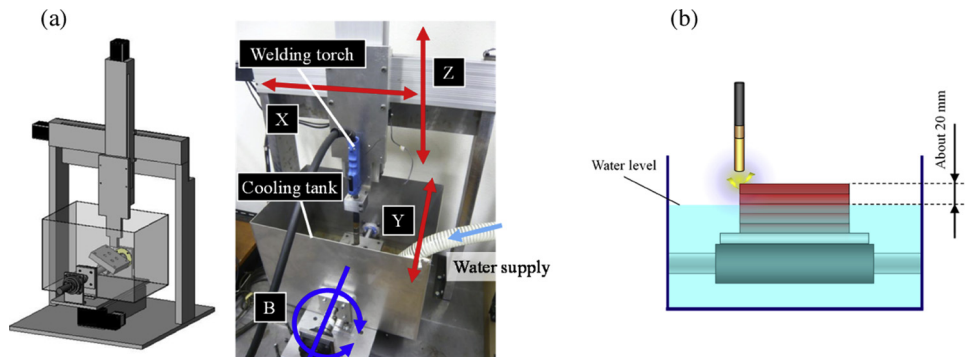

Fig. 2. WAAM system (a) Fabrication machine constructed with four axes (b) Fabrication with water cooling.
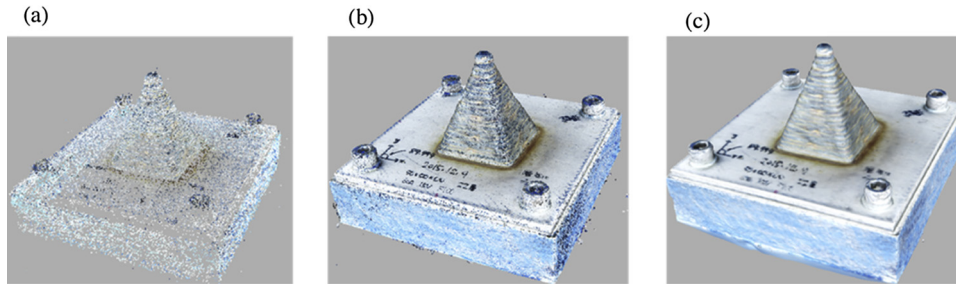
Fig. 3. SfM process for a fabricated object (a) Sparse point cloud (b) Dense point cloud (c) 3-D shape data.
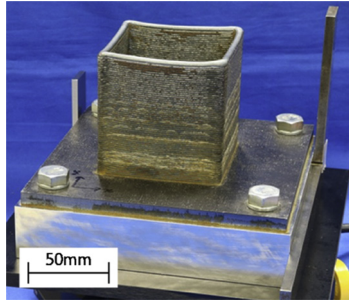

Fig. 4. Measurement object.

models do not have any information about the scale or direction; hence, it is necessary to input the geometric information or quantitative values of the camera positions [17]. In this study, the known coordinate values were input into the feature points before generating the "sparse point cloud."

2.3.2. Measurement equipment and conditions for SfM

The measurement object shown in Fig. 4 is a wall structure with a square bottom face with a side length of about 70 mm and a height of 80 mm. A substrate with a thickness of 10 mm was fixed on the reference block. Two squares were set at the corner of the reference block. The coordinate values of their vertices were measured as quantitative values to create the SfM model with information about the scale. About 30 points per wall of the fabricated object were measured using a contact coordinate measuring machine (CMM, Mitutoyo Crysta-Plus M776). The minimum distance between a point measured by the contact CMM and the mesh on SfM model was defined as the measurement error as shown as Fig. 5; the average value of all the measurement results was taken as the representative value.

The photography apparatus shown in Fig. 6 was used to acquire photographs from several angles. The fabricated object was set at the center of a turntable with CNC. By controlling the rotation angle of the turntable at equal intervals, images of the fabricated object for one revolution could be acquired without changing the attitude of the camera. To only change the attitude of the fabricated object, the background was always the same, making masking processes easy. After acquiring the images for one revolution, the attitude of the camera was changed, and photographs were again acquired at different angles. Overall, images for two revolutions with different acquisition angles were acquired. The photography conditions and camera specifications and are listed in Tables 2 and 3, respectively. The light environment was a fluorescent lamp mounted on a ceiling in a laboratory. In the SfM process for WAAM fabricated objects, it is important to obtain images with appropriate brightness; the environment should not too dark or have halation. Therefore, the shutter speed and diaphragm value were adjusted instead of setting the light environment.

2.4. Software developed to compare the designed 3-D CAD and measured models

A software program that could validate the positional relation between the SfM and 3-D CAD models and could modify the work origin to ensure that the thickness of each inclined wall is constant was developed. The software program for modifying the work origin is based on open-source point-cloud data processing called the Point Cloud Library. The Point Cloud Library is based on the C++ language and implements a plethora of point-cloud registration algorithms for both organized an unorganized dataset. It identifies the corresponding points between two models and finds a transformation that makes the distance constant. This process is repeated because the correspondence search is affected by the relative position and orientation of the datasets. Once the alignment errors fall below a given threshold, the registration is said to be complete. Through these processes, the work origin was corrected to enclose the 3-D CAD model within an SfM model. In addition, the
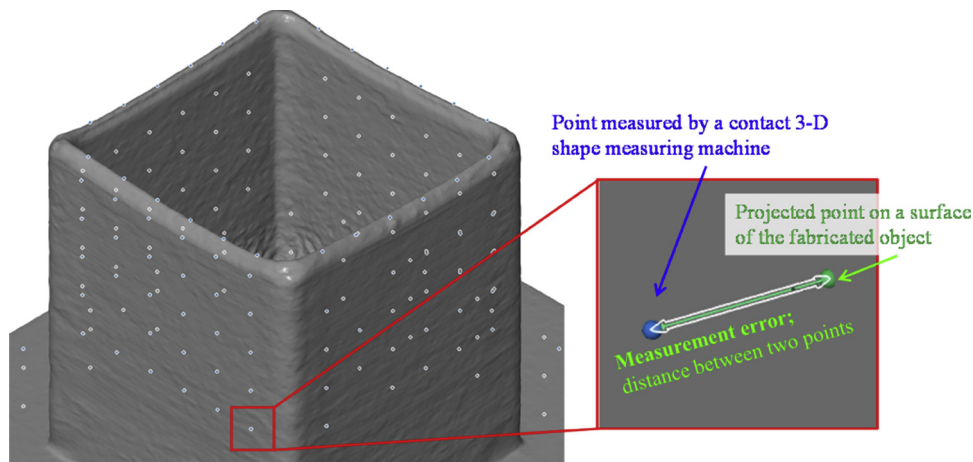

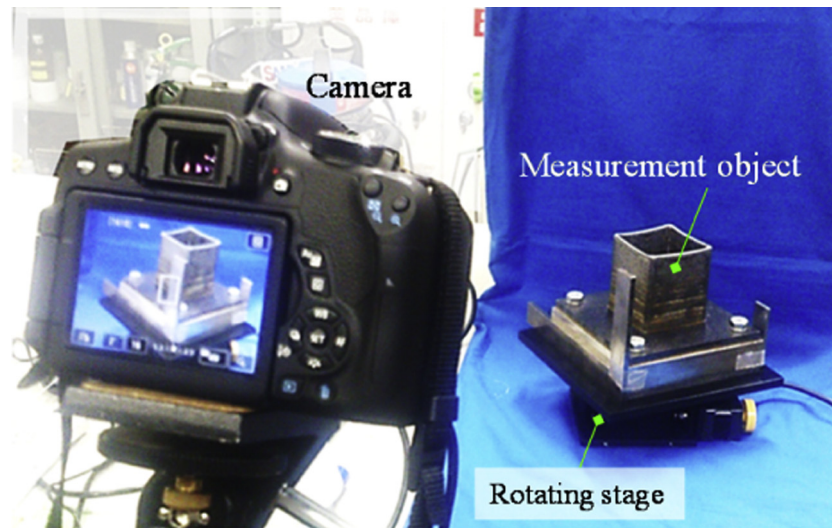
Fig. 5. Definition of measurement error in a SfM process.

Fig. 6. Photography apparatus.

Table 2
Photography conditions.

		First	Second
Subject distance L	cm	80	80
The height of the camera H	cm	141	123
The height of the rotating table h	cm	73	
Depression angle θ	deg.	58	39
Number of shots		60	60
F-number		16	
Shutter speed	sec	2	
ISO speed		400	

Table 3
Specifications of the camera used.

Camera No.		Canon EOS Kiss X8i
Effective pixels	pix	24 M(6000 × 4000)
Focal length	mm	36
Imaging element size	mm²	22.3 × 14.9 CMOS

operator could visually verify the relative location by post-processing since the modified SfM model had a color distribution; red or yellow indicated where the two models were close, and blue or purple indicated where they were quite separated. It is possible to make slight manual adjustments if automatic modification is not sufficient.

2.5. Optimization of material removal and thickness of each wall in finish machining by the developed software

In Section 3, the effectiveness of the developed software comparing the 3-D CAD data and SfM model is demonstrated by the following

process. The target shapes in the case study are a hollow quadrangular pyramid (Section 3.2) and hollow turbine blade (Section 3.3). These SfM models were generated from 120 images acquired by the photography apparatus presented in Section 2.3.2. The SfM model and CAD data of the fabricated objects were input into the developed software, and the original work design was modified to ensure that the thickness of each wall was about the same.

The final shape of the hollow quadrangular pyramid has a square bottom face with a side length of 33 mm and a height of 40 mm in the Z + direction. Moreover, the substrate and unmachined parts were completely removed, and only the WAAM-fabricated object became the final product after finish machining (Case A in Section 1). In the WAAM process, the hollow fabricated object was accumulated along a path that accumulated a hollow quadrangular pyramid that has a square bottom face with a side length of 50 mm and a height of 60 mm. To emphasize that the part with a height of 40 mm was finished from the fabricated object with a height of 60 mm, the unmachined and substrate parts were not removed. The work origin was automatically modified along the X, Y, and Z directions to ensure that the thicknesses of the four inclined walls were constant. The quadrangular pyramid has a square bottom face with a side length of 50 mm, a height of 60 mm, and a closed shape in the Z + direction. The work origin was manually modified along the Z direction to decrease the amount of material removed during the cutting process (Fig. 7). The amounts of material removed from the four inclined walls without and with modification of the work origin were calculated from the difference between the volumes of the CAD and SfM models. The SfM model was divided into four parts along the 45° and -45° directions through the apex of the 3-D CAD model. Then, the inclined walls along the Y-, X-, Y +, and X + directions were defined as Front, Left, Back, and Right, respectively (Fig. 8).

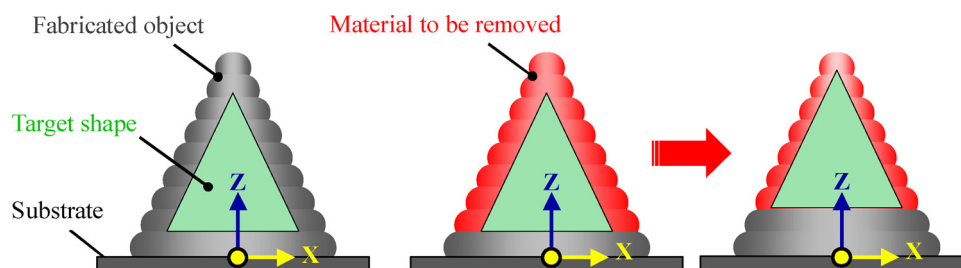To evaluate whether the four inclined wall thicknesses with

Fig. 7. Movement of the target shape along the Z + direction to decrease the amount of material removed.
(a) Original position (b) Material removed without modification (c) Material removed with modification along the Z + direction
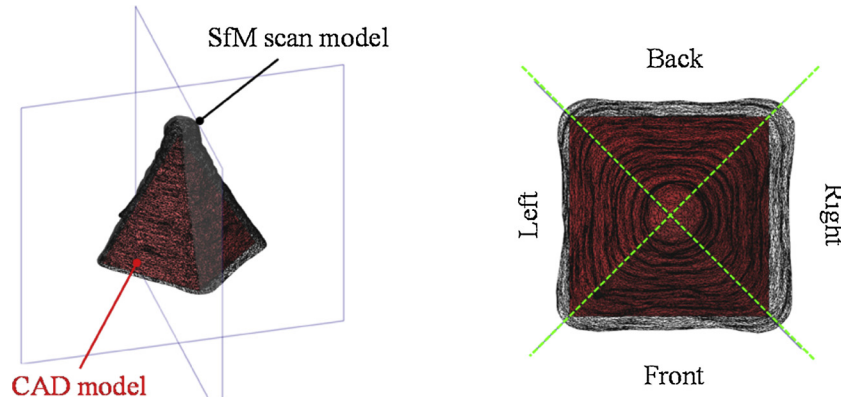
Fig. 8. Material removed from the four inclined walls (a) Whole view (b) Top view.
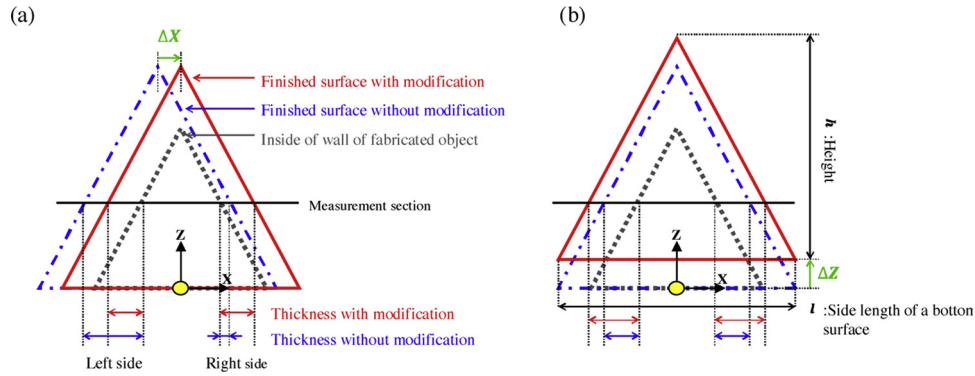

Fig. 9. Schematic of the thicknesses without and with modification of a work origin.
(a) Modification along the X direction (b) Modification along the Z direction

modification were uniform, they were measured with a noncontact 3-D shape measuring machine (Keyence VR-3000) after the fabricated object was cut in two. The thicknesses without modification were estimated from the modification based on the modification of the work origin and inclined wall thicknesses. The modification of a work origin along X, Y, and Z axis are ΔX, ΔY, and ΔZ, respectively. Fig. 9(a) shows the thicknesses of the inclined walls of the left and right side without and with modification along X axis. The thickness of Left without the modification is equal to the one with the modification added ΔX, and that of Right without modification is equal to the one with the modification subtracted ΔX. Fig. 9(b) shows the thicknesses of Left and Right without and with modification along Z axis. The modification of a work origin along the Z + direction increases the thicknesses of all inclined walls because of the quadrangular pyramid with a closed shape in the Z + direction. The height and the width of a bottom surface of the quadrangular pyramid are h and l, respectively. The thicknesses of Left, Right, Front, and Back without modification are L_t, R_t, F_t, and B_t, respectively. In addition, with modification they are L_t', R_t', F_t', and B_t', respectively. L_t, R_t, F_t, and B_t are given as follows:

$$L_t = L_t' + \Delta X - \Delta Z \times l/h \tag{1}$$

$$R_t = R_t' - \Delta X - \Delta Z \times l/h \tag{2}$$

$$F_t = F_t' + \Delta Y - \Delta Z \times l/h \tag{3}$$

$$B_t = B_t' - \Delta Y - \Delta Z \times l/h \tag{4}$$

The final shape of the hollow turbine blade was fabricated on existing material with a rectangular parallelepiped shape. The existing material was also handled as part of the final product (Case B in Section 1). The work origin was automatically modified and shifted along the X and Y axes. The uniformity of the wall thickness was evaluated by the maximum and minimum distances between the SfM and CAD models because it was difficult to measure the wall thickness of the twisted turbine blade. The maximum and minimum distances without and with the modification of the work origin were calculated from the mesh distance corresponding to the SfM and CAD models (Fig. 10).

3. Results and discussion

3.1. Measurement accuracy of SfM

The modeling results obtained by SfM are shown in Fig. 11. Compared with the reference block, the modeling accuracy of the fabricated shape is higher. The number of the feature points extracted from the reference block decrease owing to the metallic luster. On the other hand, the object fabricated with the WAAM process has irregular bumpy surfaces with a random pattern due to melting, solidification, and oxidation. To extract a large number of feature points from the surface, a SfM model with a high accuracy should be successfully constructed.

Fig. 12 shows the relationship between the number of images for SfM and the average measurement accuracy. The error bars show the standard deviation. The measurement errors are 0.26 ± 0.22, 0.16 ± 0.16, 0.14 ± 0.13, and 0.13 ± 0.11 mm for 20, 40, 60, and 120 images, respectively. As the number of images increases, the measurement error decreases and converges. In addition, the measurement error for 20 images is relatively large; however, the measurement error for 40, 60, and 120 images is approximately equal.

The results of the measurement accuracy of SfM are for the WAAM fabricated object composed of mild steel with dimensions of approximately $100\,mm \times 100\,mm \times 100\,mm$. The measurement accuracy of SfM differs when a large fabricated object or object with metallic luster is targeted. When placing a large fabricated object within a
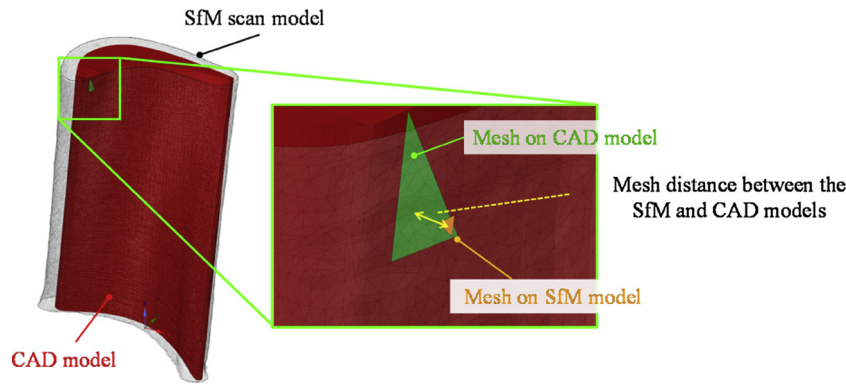
Fig. 10. Maximum and minimum distances between the SfM and CAD models without and with modification of the work origin.
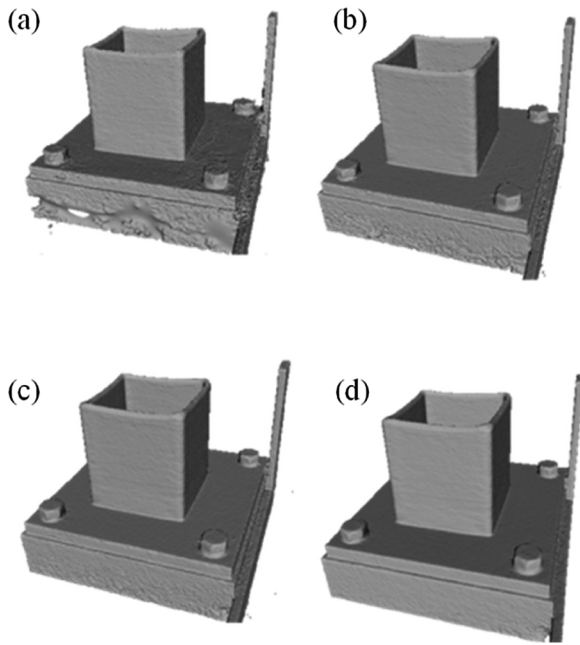

Fig. 11. Modeling results obtained by SfM (a) 20 images (b) 40 images (c) 60 images (d) 120 images.
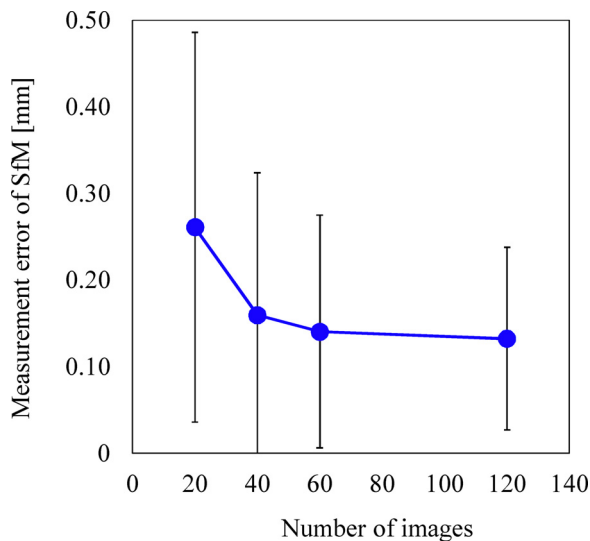

Fig. 12. Modeling results obtained by SfM.

photographic viewing angle, the pixel resolution is lower than that of the smaller one; therefore, the measurement accuracy of SfM is lower for a large object. It is considered that the measurement accuracy of SfM can be improved by setting multiple different shooting positions along the vertical direction and acquiring multiple images that overlap 60% or more. When a fabricated object with metallic luster is targeted, such as a titanium object fabricated in a chamber in an argon atmosphere, there is a possibility that the measurement accuracy is not sufficiently high because it is difficult to extract a large number of feature points from the surface. In this case, a random pattern must be added on the surface of a fabricated object using spray. Thus, the metallic luster of the fabricated object is reduced, and a large number of feature points can be extracted from the surface; therefore, the measurement accuracy of SfM is improved. The relationship between measurement accuracy, camera method to acquire images, and modeling time must be addressed in a future study.

3.2. Case study 1: Hollow quadrangular pyramid

3.2.1. Amount of material removed

Fig. 13(a) shows the fabricated quadrangular pyramid with a square bottom face with a closed shape in the Z + direction. The amount of material removed could be reduced by offsetting the work origin along the Z + direction. The actual fabricated object had 22 layers and a height of 65 mm. The top 40 mm of the fabricated object was finished by milling to prevent the cutting tool from interfering with the substrate and screw head. The photography conditions are listed Table 4. The system was used to compare the models constructed by SfM (Fig. 14) and the 3-D CAD designed model and then make the amount of material removed from each inclined wall uniform. Finally, it translated the original SfM model, including the 3-D CAD model, into a newly developed SfM model. Fig. 15(a) shows the run-time state. As seen on the left side in red, the 3-D CAD model was located closer to the X- direction compared with the SfM model. The position of the fabricated object was shifted in the negative direction on the X axis because of the shifting of the welding point. In this study, the work coordinate in WAAM process was determined on the basis of the center of the welding torch used. However, the welding wire from the welding tip was curved slightly because the extension of the welding wire was 15 mm. Therefore, the welding point where the arc was generated and molten metal was dropped from the wire tip was different from the center of the welding torch. The surface of the 3-D CAD model was the exposed outer surface of the fabricated object, which implied that there was an uncut region after the cutting. Therefore, the work origin was automatically modified along the X and Y directions to ensure that the thickness of each inclined wall was constant without any uncut region after finishing. Moreover, the work origin was manually modified along the Z direction to decrease the amount of material removed during the cutting process. In practical terms, the original workpiece design was modified 1.52 mm
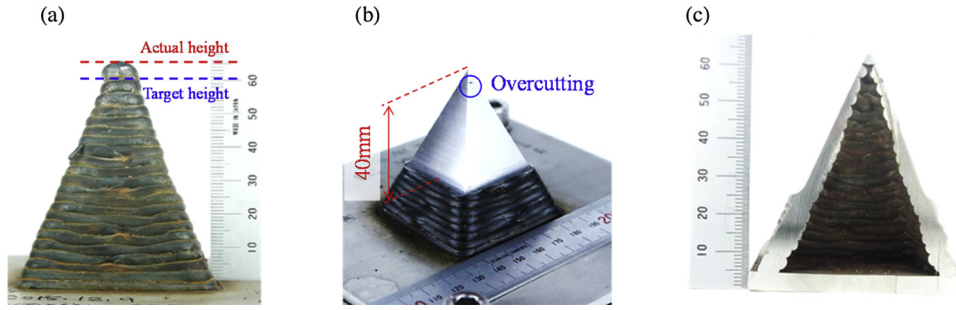
Fig. 13. Hollow quadrangular pyramid (a) Fabricated object (b) With cutting (c) Cross-sectional view.

Table 4
Photography conditions.

		First	Second
Subject distance L	cm	45	50
The height of the camera H	cm	102	108
The height of the rotating table h	cm	77	
Depression angle θ	deg.	20	30
Number of shots		60	60
Camera No.		Canon PowerShot G1 X MarkII	
F-number		16	
Shutter speed	sec	2	
ISO speed		400	

Fig. 14. SfM model.

Fig. 16. Amount of material removed from each side of quadrangular pyramid \.

X + and Y- directions. Additionally, the work origin was modified along the Z + direction so that the amount of material removed from each wall decreased. As a result, the amounts of material removed from Front, Back, and Right sides were decreased, and that from the Left side was almost same. The total amount of material removed was 25.5% less than without modification.

3.2.2. Thickness of the inclined wall

The top 40 mm of the fabricated object was finished by milling, as shown Fig. 13(b). The fabricated object did not have any uncut parts remaining. Nevertheless, overcutting occurred at the top. SfM cannot measure the internal shape of a closed object; therefore, the inside of the shape was approximately estimated from the external shape and bead width. Fig. 13(c) shows a cross section of the fabricated object, indicating that the wall thickness decreases along the Z + direction because the inclined sides had a smaller inclination angle than the target sides. In addition, there was a large cavity around the top, contrary to the estimate. According to these results, overcutting occurred, despite the decrease in the amount of material removed.
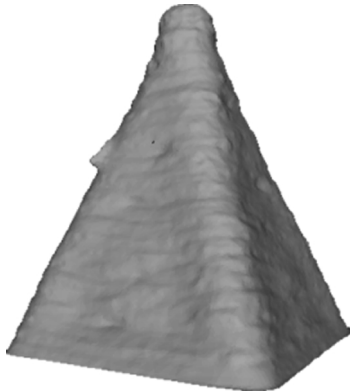
In this section, the origin for the Z axis is defined on the bottom

along the X axis, -0.54 mm along the Y axis, and 2.0 mm along the Z axis. Fig. 15(b) shows the state after the system optimized the amount of material removed; the color distributions of each inclined wall are approximately identical. The thickness of each inclined wall could be predicted to be generally constant after finishing. The amounts of material removed from the four side walls are shown in Fig. 16. It is predicted that the amount of material removed from Front and Right sides are decreased. Similarly, of the amount of material removed from Back and Left sides are increased to modify the work origin along
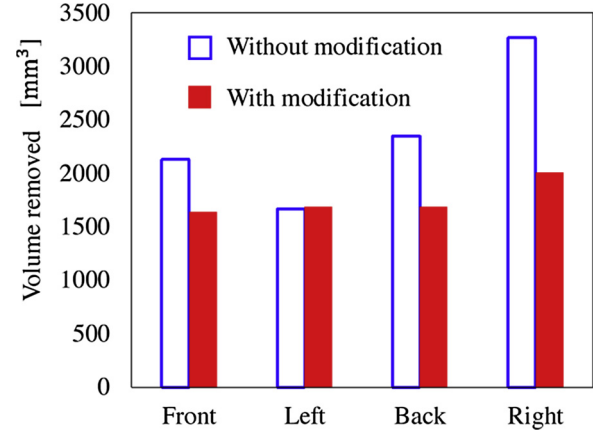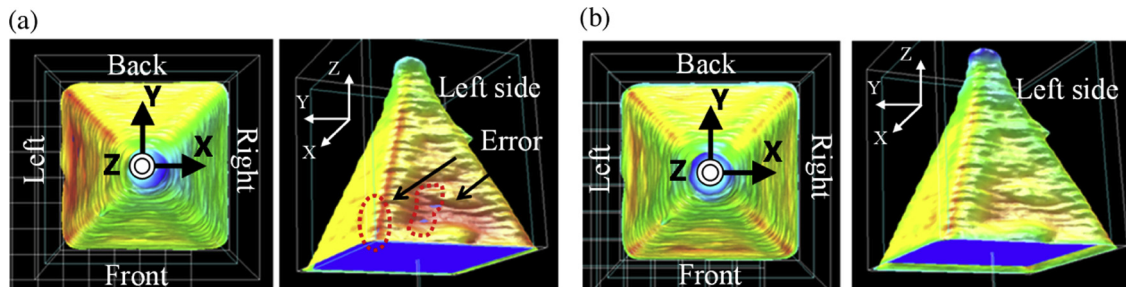

Fig. 15. Modification of the work origin (a) Without modification (b) With modification.
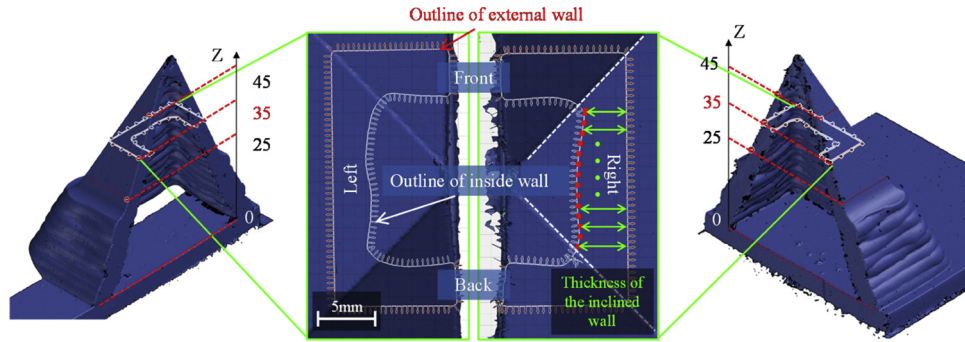
Fig. 17. Cross section and outline of an inside wall after finish machining for Z = 35 mm.
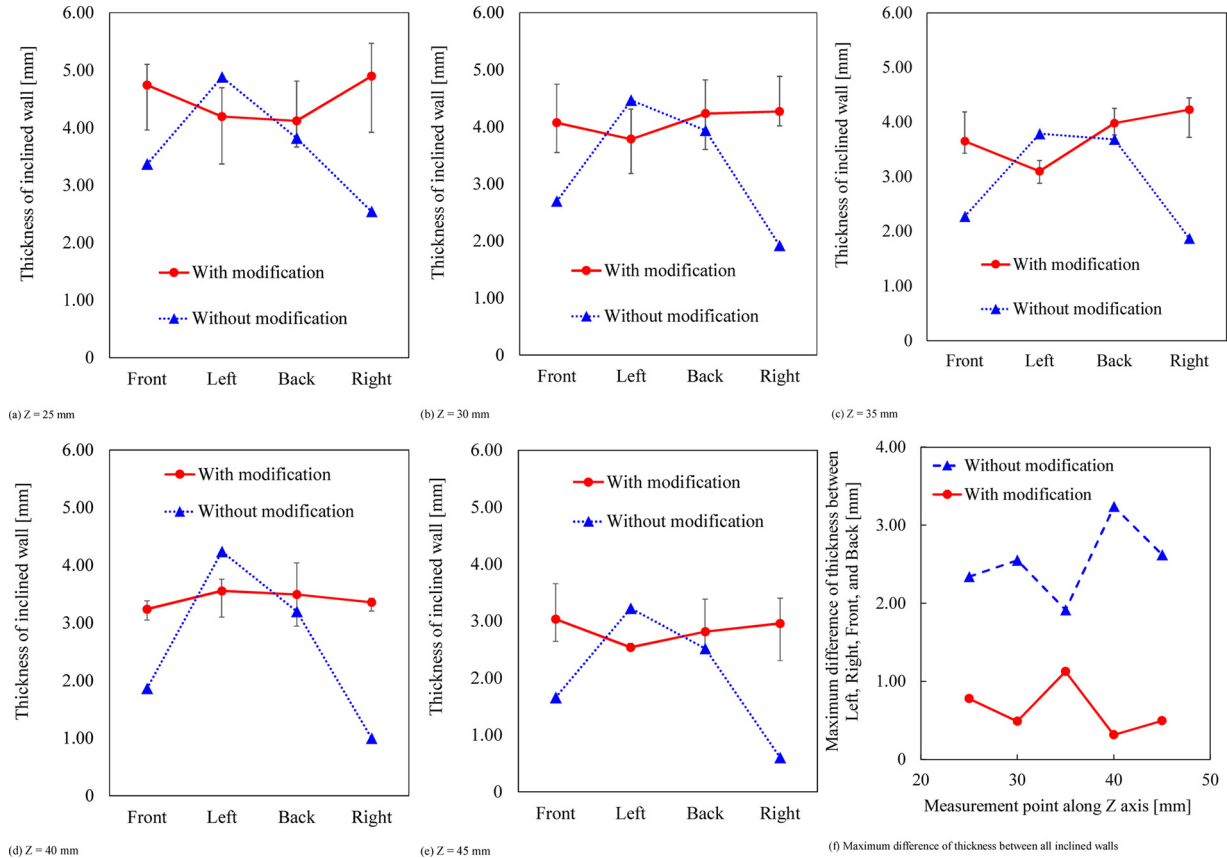

Fig. 18. Measurement results for the thickness of inclined wall.
(a) Z = 25 mm (b) Z = 30 mm (c) Z = 35 mm (d) Z = 40 mm (e) Z = 45 mm
(f) Maximum difference of thickness between all inclined walls

surface of the substrate. The direction of the Z axis is defined as the normal direction from the bottom surface of the substrate. The measurement cross sections were located at Z = 25, 30, 35, 40, and 45 mm. A cross section for Z = 35 mm is shown in Fig. 17. The distance between the inside wall and the cutting surface was measured at 1 mm intervals, and their average was defined as the thickness of the wall. As indicated by the results in Fig. 18(f), the differences between the thicknesses of different surfaces decrease with modification. For Z = 40 mm, the maximum difference between the thicknesses was 3.24 mm without modification and could be reduced to 0.32 mm as shown in Fig. 18(d). Fig. 18 shows that the thickness of Back without modification is greater than that of the Front, and their maximum of difference is 1.41 mm for Z = 35 mm. In addition, the thickness of Left without modification is considerably greater than that of Right, and their maximum difference is 3.24 mm for Z = 40 mm; the difference without modification is because of the curve of the tip of the wire as

indicated in 3.2.1. The difference in the wall thickness with modification was approximately 1 mm because of the unmachined surface of the inside wall with a large irregularity. As shown in Fig. 17, the middle and corner of the inside walls are convex and concave, respectively, because the inclined walls have an overhang shape. To begin the process, molten metal was dropped onto the overhang on the wire. WAAM is largely influenced by gravity; hence, the internal surface tends to be rougher than the estimated surface. For Z = 35 mm, the maximum and minimum thickness of the inclined wall was 4.44 mm and 3.72 mm, respectively. Therefore, it is considered that the thickness of the inclined wall is within the scope of the assumptions for the objective of this research.

3.3. Case study 2: Hollow turbine blade

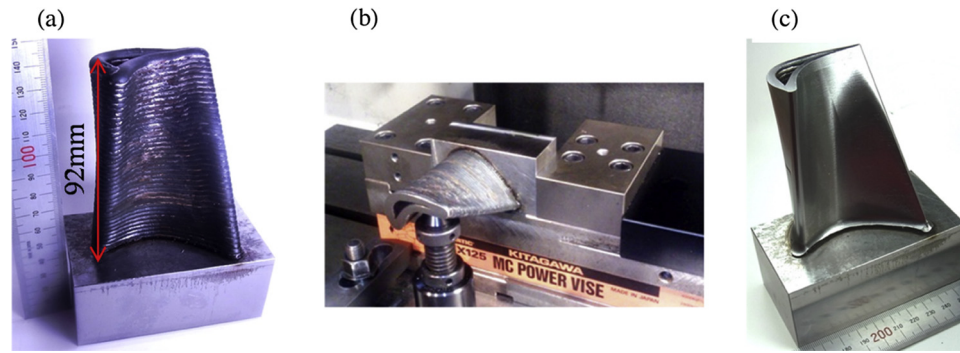The target shape is shown in Fig. 19(a) and is a 90-mm-high turbine

Fig. 19. Fabrication of hollow turbine blade shape.
(a) Fabricated object (b) Mounting on a machining center in the finishing process (c) After finishing
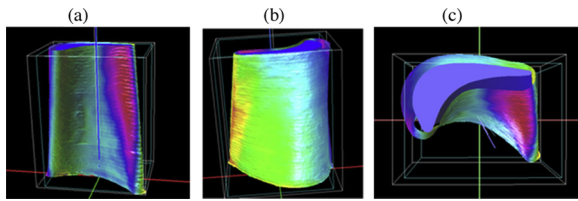

Fig. 20. Difference between the fabricated object surface and the 3-D CAD model without modification of the work origin (a) Front view (b) Back view (c) Top view.

Fig. 21. Difference between the fabricated object surface and the 3-D CAD model with modification of the work origin (a) Front view (b) Back view (c) Top view.

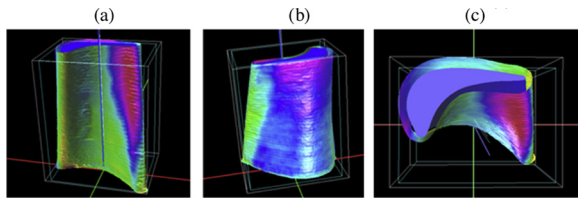blade with a twisted overhang; thus, the torch feed speed was adjusted for each part for the horizontal fabrication of each layer. The actual fabricated object had a height greater than 90 mm. Therefore, the mesh in the top part of the SfM model was deleted to make the height 90 mm, and the SfM model was compared with the 3-D CAD model designs using the system described above. Fig. 20 shows the run-time state without modification, and the minimum and maximum distances between these models were 0.27 and 6.60 mm, respectively. Because the edges of the turbine blade were red and yellow, the fabricated object was located close to the X- direction. Then, the original workpiece was automatically modified -1.18 mm along the X axis and -0.93 mm along the Y axis. The color distributions of the turbine blade were more uneven compared with those of the quadrangular pyramid, as shown in Fig. 21. The turbine blade with a twisted overhang was fabricated several millimeters higher than the target height. The fabricated object was lengthened along the Z + direction so that the distances between both models were comparatively uneven. With modification, the minimum and maximum distances were 0.77 and 5.51 mm, respectively. Therefore, the thickness of the fabricated object after cutting could be predicted to be more constant than that without modification. In the finishing process, fabricated objects were milled with a machining center (MAZAK, VCN-410A), as shown Fig. 19(b). Fig. 19(c) shows the fabricated object after cutting. The turbine blade, which was constructed of freeform surfaces, was machined to be similar to the target shape. With the cooperative system developed in this research, we confirmed whether or not uncut parts remained after fabrication by

WAAM. The system optimized the amount of material removed, and the target shape was rapidly cut.

4. Conclusions

In this study, we developed a system to optimize the amount of material removed during the cutting process of objects fabricated by WAAM. This system compared a model constructed by SfM with the designed 3-D CAD model and then regularized each surface by translating the original SfM model to include the 3-D CAD model. The measurement accuracy of the fabricated object with SfM was investigated. The thickness of each inclined wall after finishing was measured. Finally, a hollow quadrangular pyramid with a closed shape and a hollow turbine blade with a twisted overhang were manufactured using the developed system. The major conclusions of this study are as follows.

(1) The measurement accuracy of SfM was investigated with a fabricated shell structure with dimensions of about 70 mm × 70 mm × 80 mm. Numerous feature points were successfully extracted from the fabricated object owing to the irregular surface with a random pattern made by the WAAM process. This caused the SfM model to be reconstructed with a high-accuracy shape. As the number of images increased, the measurement error decreased. The minimum measurement error was 0.13 ± 0.11 mm with 120 images, and the maximum measurement error was 0.26 ± 0.22 mm for 20 images. Consequently, the measurement accuracy of the 3-D data of SfM was within an acceptable range for the WAAM process and finish machining.

(2) The developed software could verify whether a target shape was enclosed within a fabricated object and automatically or manually modify the work origin to ensure that the thickness of each inclined wall was constant. For a hollow quadrangular pyramid with a square bottom face with a side length of 50 mm and a height of 60 mm, the work origin was modified along the X, Y, and Z directions using software. As a result, the total amount of material removed could be reduced to 25.5% of that without modification. In addition, the differences between the thicknesses of different surfaces decreased with modification. In particular, the maximum difference between thicknesses was reduced from 3.24 mm without modification to 0.32 mm.

(3) With the cooperative system for WAAM and machining, a turbine blade with a twisted overhang was fabricated and finished with a milling process. The target shape was successfully machined without any defects.

(4) In the future work, the WAAM system is further developed such that the measurement results of a fabricated object and the modification of the work origin are provided as feedback to the fabrication strategy, thereby improving the shape accuracy of objects

fabricated using the WAAM process. This will ensure that the amount of material used is optimized and wastage is reduced. Moreover, the thin-wall parts can also be fabricated without over-cutting, voids, and uncut regions.

Acknowledgment

References

[1] T. Wohlers, Wohlers Report 2017, Wohlers Associates Inc, Fort Collins, 2017.

[2] A.R. McAndrew, M.A. Rosales, P.A. Colegrove, J.R. Hönnige, A. Ho, R. Fayolle, K. Eyitayo, I. Stan, P. Sukrongpang, A. Crochemore, Z. Pinter, Interpass rolling of Ti-6Al-4V wire + arc additively manufactured features for microstructural refinement, Addit. Manuf. 21 (2018) 340–349, https://doi.org/10.1016/J.ADDMA.2018.03.006.

[3] H. Takagi, H. Sasahara, T. Abe, H. Sannomiya, S. Nishiyama, S. Ohta, K. Nakamura, Material-property evaluation of magnesium alloys fabricated using wire-and-arc-based additive manufacturing, Addit. Manuf. 24 (2018) 498–507, https://doi.org/10.1016/J.ADDMA.2018.10.026.

[4] K. Tanaka, T. Abe, R. Yoshimaru, H. Sasahara, Strength of manufactured object made by direct metal lamination using arc discharge, Japan Soc. Mech. Eng. 79 (2013) 1168–1178 (accessed January 22, 2019), https://www.jstage.jst.go.jp/article/kikaic/79/800/79_1168/_pdf/-char/ja.

[5] T. Abe, H. Sasahara, Dissimilar metal deposition with a stainless steel and nickel-based alloy using wire and arc-based additive manufacturing, Precis. Eng. 45 (2016) 387–395, https://doi.org/10.1016/j.precisioneng.2016.03.016.

[6] J.N. Dupont, A.R. Marder, The effect of welding parameters and process type on arc and melting efficiency is evaluated, Weld. Res. Suppl. (1995) 406–416 https://canteach.candu.org/Content Library/20053408.pdf (accessed January 22, 2019).

[7] D. Ding, Z. Pan, D. Cuiuri, H. Li, Wire-feed additive manufacturing of metal components: technologies, developments and future interests, Int. J. Adv. Manuf.

Technol. 81 (2015) 465–481, https://doi.org/10.1007/s00170-015-7077-3.

[8] R.R. Unocic, J.N. Dupont, Process efficiency measurements in the laser engineered net shaping process, Metall. Mater. Trans. B 35B (2004) 143–152 (accessed January 22, 2019), https://link.springer.com/content/pdf/10.1007%2Fs11663-004-0104-7.pdf.

[9] Y. Ogino, Y. Takabe, Y. Hirata, S. Asai, Numerical Model of Weld Pool Phenomena With Various Joint Geometries and Welding Positions*, (2017) (accessed October 12, 2017), https://www.jstage.jst.go.jp/article/qjjws/35/1/35_13/_pdf.

[10] J. Xiong, Y. Lei, H. Chen, G. Zhang, Fabrication of inclined thin-walled parts in multi-layer single-pass GMAW-based additive manufacturing with flat position deposition, J. Mater. Process. Technol. 240 (2017) 397–403, https://doi.org/10.1016/j.jmatprotec.2016.10.019.

[11] Y. Ogino, S. Asai, Y. Hirata, Numerical simulation of WAAM process by a GMAW weld pool model, Weld. World 62 (2018) 393–401, https://doi.org/10.1007/s40194-018-0556-z.

[12] J.S. Panchagnula, S. Simhambhatla, Manufacture of complex thin-walled metallic objects using weld-deposition based additive manufacturing, Robot. Comput. Manuf. 49 (2017) 194–203, https://doi.org/10.1016/j.rcim.2017.06.003.

[13] D. Ding, Z. Pan, D. Cuiuri, H. Li, A multi-bead overlapping model for robotic wire and arc additive manufacturing (WAAM), Robot. Comput. Manuf. 31 (2014) 101–110, https://doi.org/10.1016/j.rcim.2014.08.008.

[14] T. Abe, H. Sasahara, Development of the shell structures fabrication CAM system for direct metal lamination using arc discharge-lamination height error compensation by torch feed speed control-, Int. J. Precis. Eng. Manuf. Technol. 16 (2015) 171–176, https://doi.org/10.1007/s12541-015-0022-4.

[15] M.J. Westoby, J. Brasington, N.F. Glasser, M.J. Hambrey, J.M. Reynolds, "Structure-from-Motion" photogrammetry: a low-cost, effective tool for geoscience applications, Geomorphology 179 (2012) 300–314, https://doi.org/10.1016/j.geomorph.2012.08.021.

[16] Y.-M. Wei, L. Kang, B. Yang, L.-D. Wu, Applications of structure from motion: a survey *, J Zhejiang Univ-Sci C (Comput Electron). 14 (2013) 486–494, https://doi.org/10.1631/jzus.CIDE1302.

[17] M. Lourakis, X. Zabulis, Accurate Scale Factor Estimation in 3D Reconstruction, in: Int. Conf. Comput. Anal. Images Patterns, (2013), pp. 498–506 (Accessed October 1, 2018), https://pdfs.semanticscholar.org/549a/ae52cb11a2fd45da4c0c3cc20a57cc38524f.pdf.